



Predicting Avalanche Danger in Northern Norway Using Statistical Models

Kai-Uwe Eiselt¹ and Rune Grand Graversen^{1,2}

¹Department of Physics and Technology, University of Tromsø

²Norwegian Meteorological Institute

Correspondence: Kai-Uwe Eiselt (kai-uwe.eiselt@uit.no)

Abstract. Snow avalanches are one of the most impactful natural hazards in mountainous areas. Thus, the assessment and forecasting of avalanche danger is of great importance for the protection of life and property. A changing climate may lead to changes in avalanche danger although the manifestation is unclear. Since climate change is regionally different, an assessment of potential avalanche danger changes should be conducted on a regional basis. Here the focus is on avalanche danger in northern Norway, i.e., a region in the Arctic. We utilise regional expert avalanche-danger level (ADL) assessments together with the 3-km Norwegian reanalysis (NORA3) to estimate the linkage between avalanche danger in the Troms region of Norway and the prevailing weather conditions represented by NORA3 as well as snow-cover information from the snow model seNorge. Both a binary and 4-level case are considered. Two random forest (RF) models are optimised and trained, one for the binary case and one for the 4-level case.

The binary-case RF model exhibits a much higher overall accuracy (76 %) than the 4-level case RF model (57 %), which is due to the latter often confusing ADLs 1 and 2 and ADLs 3 and 4. Still, the missclassification difference is almost never larger 1 ADL and the distribution of the frequencies of the different ADLs is reproduced. The most important predictive features of avalanche danger found here are broadly consistent with earlier studies and are mostly related to new snow and wind accumulated and averaged over several days. The binary-case RF model is used to hindcast binary-case avalanche activity (BCA) from 1970 to 2023. In this period, the spring season (Mar-May) shows a small but in most regions significant increase in BCA, whereas the winter season (Dec-Feb) exhibits mostly non-significant negative trends. Moreover, BCA is found to be correlated with the Arctic Oscillation (AO) index especially in winter, although this correlation may have deteriorated in recent years. Given recent advances in skill of representing the AO in decadal prediction systems this is an encouraging result for the predictability of future avalanche danger tendencies in northern Norway.

The methodology presented here may be generally applied to link climate indicators to numerical climate model output, enabling their prediction for future climate change scenarios.

1 Introduction

Environmental and climate indicators associated with, e.g., natural hazards and human activities, both on land (e.g., the danger of avalanches or landslides) and at sea (e.g., changes in nutrient concentration or stratification essential for fishery), represent



25 important information when it comes to society planning and policy-making, especially under changing conditions. Prediction
of these indicators, for instance avalanches that are a large risk to life and property, is of great importance, especially in densely
populated areas or tourism “hot-spots”. Other environmental indicators, such as nutrient concentration may be related more to
the conditions for industry, farming, and fishery and are thus strongly important for the planning of these industries and their
infrastructure (e.g., agricultural and marine-spatial planning). However, because of the great complexity of the environment
30 in which these indicators emerge, they are often not *directly* modelled, implying a paucity of information and hampering of
planning for the present and especially the future. Nonetheless, some information may be inferred *indirectly*, i.e., from other
environmental properties that *are* directly modelled. This may be done using statistical methods that quantitatively relate the
indicator in question to the modelled properties. One type of such properties for which a rich pedigree of direct modelling as
well as observational monitoring exist is meteorological weather data. Thus, this data and its changes are often used to infer
35 knowledge about—and changes in—indicators that are not directly modelled. An important benefit of this is that a diverse set
of modelled future scenarios exists for meteorological data. This offers the opportunity to investigate potential future changes
of environmental parameters based on the modelled future changes in weather conditions.

One environmental indicator that is associated with natural hazards and that is related to meteorological parameters is snow
avalanche danger or hazard (e.g., Statham et al., 2018). The terms danger and hazard are synonyms (e.g., Statham, 2008), but
40 according to Müller et al. (2016a), the former is more often used in Europe, while the latter is more typical in North America.
In the following, avalanche danger is used.

Avalanche danger aggregates information about the likelihood of occurrence as well as the size of avalanches to a single
integer—the avalanche danger level (ADL; e.g., Müller et al., 2016b). A standardised 5-level ADL scale was agreed upon
by the European Avalanche Warning Services (EAWS) in 1993 and subsequently (in 1997) adopted in North America as well
45 (e.g., Schweizer et al., 2020). The ADL is typically forecast regionally by a team of experts based on (1) snowpack stability, (2)
the frequency of snowpack stability, and (3) avalanche size (e.g., Müller et al., 2023). As Pérez-Guillén et al. (2022) note, this
means that ADL forecasting still follows the approach already described by LaChapelle (1980). Nonetheless, in recent years
advances have been made in incorporating physical (snowpack) modelling in the forecast (Morin et al., 2020). Moreover, in
Switzerland an approach relying exclusively on machine learning models (i.e., without expert input as, e.g., in Schweizer and
50 Föhn, 1996) to predict regional ADL with promising accuracy rivalling that of human experts (see, e.g., Techel and Schweizer,
2017) has been developed (Pérez-Guillén et al., 2022) and is about to be implemented operationally (Maissen et al., 2024).
Employing machine learning to robustly predict ADL offers the possibility of (1) hindcasting and potentially connecting ADL
to known climate patterns, (2) quicker and more fine-resolution predictions of ADL based on numerical weather forecasts
and (3) prediction of ADL based on numerically modelled future climate-change scenarios. The latter is highly important for
55 future planning for stakeholders (e.g., ski-tourism industry or infrastructure departments) as a changing climate likely impacts
avalanche occurrence and danger (e.g., Castebrunet et al., 2014; Laute and Beylich, 2018; Dyrrdal et al., 2020; Mayer et al.,
2024).

While exact deterministic prediction of avalanche release will likely remain out of reach for the time being (Schweizer
et al., 2003; Dkengne Sielenou et al., 2021), the possibility of using weather data to forecast avalanches was recognised



60 decades ago (e.g., Atwater, 1954; LaChapelle, 1966). In the years since, many studies have focused on statistical prediction of
avalanche occurrence from meteorological data (e.g., Judson and Erickson, 1973; Bakkehøi, 1987; Davis et al., 1999; Kronholm
et al., 2006; Jomelli et al., 2007; Jaedicke et al., 2008; Hendriks et al., 2005, 2014; Gauthier et al., 2017; Mayer et al., 2023;
Viallon-Galinier et al., 2023; Hao et al., 2023). These studies are based on observational avalanche records and typically focus
on small regions with strong observational coverage. As observational records for larger regions are likely incomplete (e.g.,
65 Schweizer et al., 2020), especially in the sparsely populated regions such as northern Norway (Jaedicke et al., 2008), direct
forecasting of the probability of avalanche occurrence for larger areas appears so far infeasible. Instead, as indicated above,
the forecasting of ADL is more promising. While there have been attempts for many years to forecast ADL with the help of
statistical methods (mostly nearest-neighbour methods; Schweizer and Föhn, 1996; Brabec and Meister, 2001), this research
has gained more momentum only in recent years (Dekanová et al., 2018; Fromm and Schönberger, 2022; Pérez-Guillén et al.,
70 2022; Blagovechshenskiy et al., 2023; Sharma et al., 2023; Maissen et al., 2024). However, e.g., the nearest-neighbour model
of Brabec and Meister (2001) based on data from 60 manual weather stations in Switzerland yielded only a 52 % prediction
accuracy. In contrast, the expert system of Schweizer and Föhn (1996), tested in the Davos region in Switzerland, achieved
up to 73 % accuracy, although only in the case where an expert was allowed to interact with the forecast. Schirmer et al.
(2009) compared several different machine learning methods to forecast avalanche danger. Notably, they also included snow-
75 stratigraphy data from simulations with the physically-based snow-cover model SNOWPACK (Bartelt and Lehning, 2002;
Lehning et al., 2002b, a). They found the best method (73 % cross-validated accuracy) to be a nearest-neighbour classifier,
which, however, included the ADL from the previous day as input. While this may improve the accuracy with respect to
daily ADL it likely deteriorates the performance for days where the ADL changes compared to the previous day (e.g., Pérez-
Guillén et al., 2022). Recently, focussing on regional dry-snow avalanche conditions in the Swiss Alps, Pérez-Guillén et al.
80 (2022) achieved the best results of predicting ADL based on meteorological and SNOWPACK-simulated snow stratigraphy
data with a random forest (RF) classifier (about 75 %). Their approach is purely data-driven and does not require expert
inputs. It may be noted that the RF model has become a generally popular method in avalanche forecasting, however it appears
to be mostly used for forecasting avalanche activity (e.g., Möhle et al., 2014; Dkengne Sielenou et al., 2021; Mayer et al.,
2023, 2024; Viallon-Galinier et al., 2023) and not ADL. Contrarily, there has been a number of studies using an artificial neural
85 network (ANN) to predict ADL in different mountain regions. However they report strongly different accuracies. For example,
Dekanová et al. (2018), using an ANN to predict avalanche danger in the Western Tatras (Slovakia) based on weather station
data, obtained accuracies of 59 to 66 %. Conversely, Blagovechshenskiy et al. (2023) reported accuracies of 77 to 91 % for
an ANN trained for the Ile Alatau Ridge in Kazakhstan. One reason for the discrepancy may be that Blagovechshenskiy et al.
(2023) use information about the snow stratigraphy as predictive features while Dekanová et al. (2018)'s information about
90 snow is confined to "actual snow depth" and "new snow depth". Furthermore, there are differences in the generation of the ADL
data set, as Blagovechshenskiy et al. (2023) had to reconstruct most of the ADLs based on actual avalanche observations while
Dekanová et al. (2018) used a historical record of ADL forecasts. Sharma et al. (2023) using the same data as Pérez-Guillén
et al. (2022) reported a best-case accuracy of 76.54 % with respect to their validation data. However, no information about the
split into training and validation data is given. This may be important because if the validation data is chosen randomly, temporal



95 correlations may cause severe overestimation of model accuracy (see section 5 below). A further reason for the comparatively
high accuracy of Sharma et al. (2023) is likely that their data was confined to dry snow avalanches. These points may explain the
discrepancy in model performance with Fromm and Schönberger (2022) who obtained an accuracy of only 48 % for an ANN
trained on meteorological and SNOWPACK-simulation data (i.e., similar to Sharma et al., 2023) for a ski-resort in the Austrian
and Swiss Alps. As test data they used one whole winter which was excluded from the training data and they considered any
100 type of avalanche. They also note that in contrast to Pérez-Guillén et al. (2022) and Sharma et al. (2023), they did not focus on
regional ADL but instead on a much smaller region, i.e., a single ski resort. The resort is strongly influenced by artificial and
intentional avalanche triggering, potentially further hampering direct comparability to the other studies.

So far, the only study investigating statistically the relation between avalanches and weather data in northern Norway is
Jaedicke et al. (2008), although this was not the main focus of that study and instead of ADL they predicted avalanche activity.
105 Moreover, Dyrørdal et al. (2020) investigated climate indices specifically related to avalanches in the Troms region in northern
Norway, but they did not statistically relate these indices to avalanche danger. In northern Norway snow avalanches are among
the most important natural hazards, causing road closures and access disruptions to towns, and casualties associated with, e.g.,
skiing, riding snowmobile, driving cars, or even being in houses. In an analysis of the Norwegian mass movement database¹
as well as Varsom², Dyrørdal et al. (2020) found that between 1730 and January 2020 in Troms, 307 casualties were caused
110 by snow avalanches. A reason for historically relatively little focus on statistical avalanche prediction in northern Norway
may be due to the sparse avalanche observations in this region (Jaedicke et al., 2008), implying that avalanche prediction
models based on observational avalanche records are likely biased. We note that the analysis in Jaedicke et al. (2008) may
suffer from this problem. To circumvent this shortcoming, we here instead rely on the expert ADL assessments published
by the Norwegian Water Resources and Energy Directorate (NVE). The ADLs are compared with a set of meteorological
115 variables which are constructed based on the 3-km Norwegian Reanalysis (NORA3). Moreover, we include several snow-
related parameters derived from the simple 1-layer snowpack model seNorge (Saloranta, 2012, 2014, 2016). seNorge is run
using daily temperature and precipitation data from NORA3 to simulate snow conditions. Like Pérez-Guillén et al. (2022), we
focus on the RF model to predict ADL in northern Norway and mostly follow their detailed model optimisation and feature
selection procedures (see section 4 below). However, we also implement an ANN with the structure suggested by Sharma et al.
120 (2023) and test its performance. But since we do not conduct an optimisation of the ANN, we include the results only in the
supplementary material (see texts S1 to S3). Generally, the RF and the ANN model yield similar results (see texts S2 and S3).

We optimise two different RF models: (1) for the original “4-level case” (ADL 5 has not been forecast in northern Norway)
and (2) for a “binary case”, where ADLs 1 and 2 and ADLs 3 and 4 are combined. Consistent with previous studies, we find
that the most important predictive features in both cases are related to accumulated new snow over several days as well as wind
125 drift. As expected, the RF model for the binary case performs much better than the model for the 4-level case, where ADLs 1
and 2 are often confused and similarly ADLs 3 and 4. The model generally over-predicts the frequencies of the medium classes
(ADLs 2 and 3) when using the balanced test data, although for the original data the class frequency distribution is reproduced.

¹<https://skredregistrering.no>

²<https://varsom.no>



Finally, using the RF model for the binary case we perform an “avalanche activity”³ hindcast for 1970–2023. While there is little general trend in avalanche activity, there is a notable peak in the 1990s, with less activity before and after. The peak in the 1990s appears to be connected to exceptionally high values of the North Atlantic Oscillation (NAO) or the Arctic Oscillation (AO) at that time. Recent advances of decadal prediction systems indicate considerable skill in representing the NAO/AO. This is encouraging as it implies a potential predictability of at least the tendency of avalanche activity on this time scale. However, we also find a decrease in correlation between NAO/AO and avalanche activity in recent years, potentially induced by other climate modes, indicating a loss of predictability. Furthermore, the influence of these climate modes on northern Norwegian avalanche activity, may confound a potential climate-change signal. If climate models simulating future climate-change scenarios are unable to represent climate modes such as NAO/AO, avalanche activity/danger projections based on these simulations may be subject to severe uncertainty.

Given the high danger posed by snow avalanches in northern Norway, an increased ability of predicting avalanche danger is of immense value to help preventing skiing accidents and fatalities in homes and on roads, as well as preparing for potential road closures and access disruptions. In the present study we attempt to make progress in this direction. It is structured as follows: Section 2 first explains the expert ADL assessments (2.1), the NORA3 reanalysis (2.2), and the seNorge model (2.3), and finally gives an overview of the avalanche-danger prediction features calculated from the NORA3 data and the seNorge output (2.4). Section 3 describes the RF model (3.1) and the employed model performance metrics (3.2). In section 4 the RF optimisation and feature selection procedure is presented and in section 5 the RF models (binary and 4-level case) are evaluated. The binary-case RF model is used in section 6 to perform a hindcast of “avalanche activity”, which is then connected to known climate patterns. Section 7 offers a summary and concluding remarks.

2 Data

2.1 Avalanche danger

In northern Norway avalanche observations are sparse and many avalanches remain undetected. Thus, using avalanche observation catalogues as training data for statistical models to predict avalanches likely introduces biases leading to incorrect or at least uncertain prediction. To avoid this potential bias, we here instead employ the daily avalanche danger level (ADL) assessment as described in section 1. In Norway the ADL assessment is generated and published⁴ by a team of experts from the Norwegian Water Resources and Energy Directorate (NVE), the Norwegian Meteorological Institute (MET), and the Norwegian Public Roads Administration (Statens vegvesen) aggregating knowledge from snow and weather observations as well as numerical weather modelling to forecast the ADL for the next couple of days. The ADL data are available from the avalanche season of 2017/18 up to present day.

³Note that our measure of avalanche activity is not based on actual avalanche observations, but is instead connected to a change in binary-case level (see section 6).

⁴The Norwegian ADLs are published at www.varsom.no.

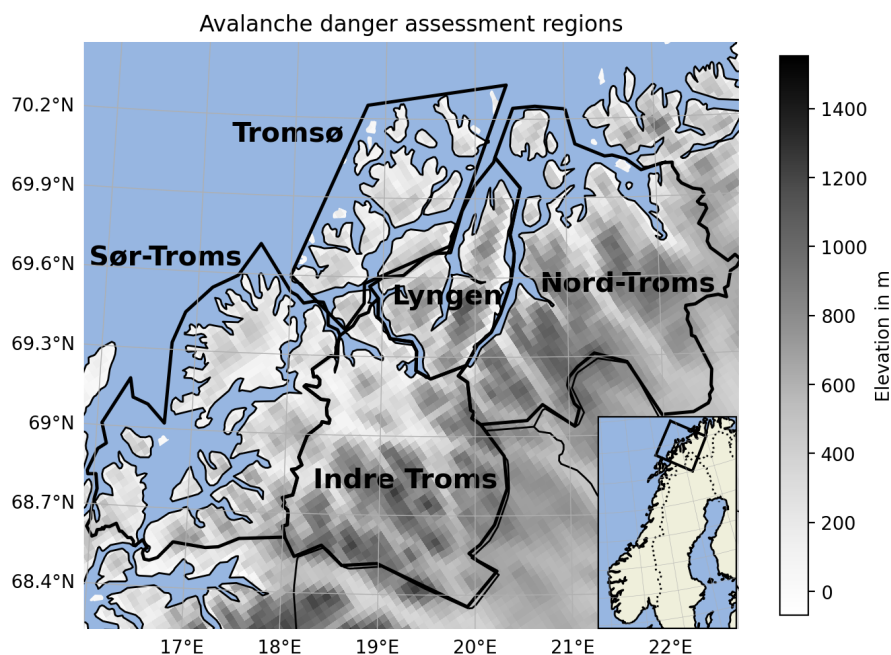


Figure 1. Study region. The black square in the inset indicates the location of the study region in Norway. The topography information is taken from NORA3.

In describing the avalanche danger by a single value per region, the ADL constitutes a large reduction in complexity. In fact, the avalanche forecaster considers several different “avalanche problems”⁵ (AP; e.g., wind slab, persistent weak layer etc.) and based on the estimated likelihood (based, in turn, on distribution and sensitivity) and size of avalanches determines a danger level per AP (Müller et al., 2023). The final ADL in a given region is taken as the highest danger level among the different APs. Hence, the ADL is a result of different APs that are related to different meteorological conditions, complicating the relation between ADL and meteorological data. However, considering only one AP reduces the amount of available data, making a robust training of statistical models more difficult. Also, at least some of the APs may be related to similar meteorological conditions and we thus believe it is still feasible to focus on the general ADL. In future work we will attempt a more detailed decomposition into the different APs.

Here, the ADLs from the northern Norwegian regions of Nord-Troms, Lyngen, Tromsø, Sør-Troms and Indre Troms are considered. The regions are depicted in Fig. 1. From Fig. 2a it is clear that there is considerable variation in frequency of the different ADLs with 2 being the most frequent and 4 the least frequent, while level 5 was never forecast in northern Norway. Hence, the ADL scale in this study is constrained to four levels. The figure also shows that the frequency of the ADLs is similar across the different regions. Conversely, the ADL frequency varies across the different recorded years (Fig. 2b), especially between levels 1 and 2. For example, in 2020 there were almost no days with level 1 but many more days with

⁵See <https://www.avalanches.org/standards/avalanche-problems/>

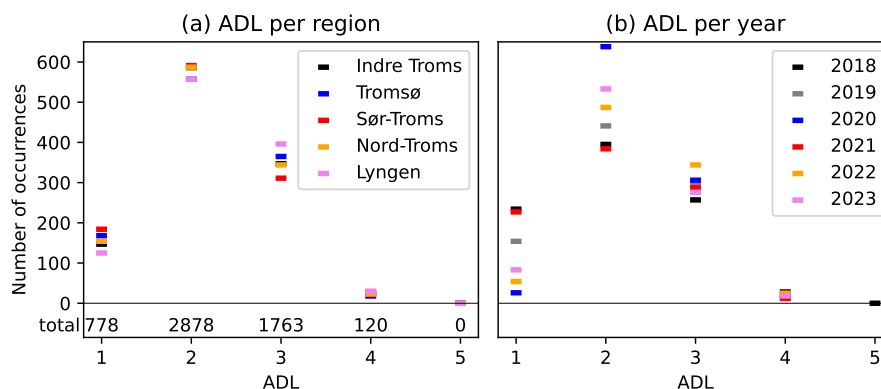


Figure 2. Summary of the avalanche danger level (ADL) data in northern Norway from winter 2017/18 to 2022/23. Note that in (b) there are more than 365 occurrences per year because the data are aggregated for all the northern Norwegian regions.

level 2. In contrast, in 2018 and 2021 there were much fewer days with level 2 and many more with level 1. The distribution of ADLs per year is important information when it comes to the splitting of training and test data for the statistical models.

As Pérez-Guillén et al. (2022) discuss, one source of noise in the ADL data is forecast error, i.e., incorrect labels. For example Techel and Schweizer (2017) find that the regional forecasts match local nowcasts only 71 % of the time. Pérez-Guillén et al. (2022) thus attempt to generate a refined subset of their ADL data by including additional information such as observational data and the outcomes of several verification studies. For northern Norway, no such verification studies exist, although there is one study trying to compare remote-sensing derived avalanche activity with forecast ADL which indicates that ADL forecasts are conservative (Eckerstorfer et al., 2017). Attempts are currently under way to increase remote-sensing coverage and detection algorithm quality, but the probability of detection has been found to depend on the type of avalanche and is overall only about 57 % (Müller et al., 2021)⁶. Furthermore, while there are in-situ observational avalanche records in northern Norway⁷ these are very sparse due to the comparatively large area and the low population density. Even using a combination of in-situ and remote-sensing observation to “tidy up” our ADL data would strongly reduce our available data so as to make robust training of a statistical model infeasible. With these reservations in mind we are here bound to use the raw ADL forecast data.

In this study, we consider two types of avalanche-danger scales. First, we employ the full ADL scale (henceforth “4-level case”). Second, we generate a binary scale (henceforth “binary case”) where the ADLs 1 and 2 are combined to binary-case level (BCL) 0 and the ADLs 3 and 4 are combined to BCL 1. This is done because (1) we find a much better model performance in predicting the binary case compared to the 4-level case (see section 5) and (2) we use the binary case in a hindcast for a rough estimate of changing avalanche activity over time and to find potential connections to known climate patterns/modes (see section 6).

⁶The Norwegian remote-sensing avalanche observations are publicly available at <https://satskred.nve.no/>.

⁷The Norwegian avalanche observations are available via Varsom Regobs (<https://regobs.no>) and NVE (<https://nedlasting.nve.no/gis/>).



2.2 NORA3

The meteorological data used in this study is taken from the 3-km Norwegian Reanalysis (NORA3). NORA3 is an atmospheric hindcast for the North Sea, the Norwegian Sea, and the Barents Sea as well as the Scandinavian Peninsula, including further parts of northern and western Europe and north-west Russia (Haakenstad et al., 2021). More precisely, it may be viewed as falling somewhere between a hindcast and a full reanalysis as it includes data assimilation only for surface parameters (Haakenstad et al., 2021; Haakenstad and Breivik, 2022). NORA3 provides a regional downscaling to a 3-km horizontal resolution of the latest version of the European Centre for Medium-Range Weather Forecasts (ECMWF) reanalysis, ERA5, with a 31-km horizontal resolution (Hersbach et al., 2020). To produce NORA3, the non-hydrostatic convection-permitting numerical weather model HARMONIE-AROME (Bengtsson et al., 2017) was run on a 3-km horizontal resolution and with 65 vertical layers, using ERA5 fields as initial and boundary conditions. At the time of writing, data availability covers the period 1970 to present day with a few months lag. It is planned to extend NORA3 back in time to 1960.

Pertinent to the present study, NORA3 has been found to significantly improve the representation of 2-m temperature, 10-m wind, and daily precipitation, particularly regarding extremes and in coastal and mountainous areas compared to its host reanalysis (ERA5) and its predecessor (NORA10; Reistad et al., 2011). These improvements appear mostly due to the higher resolution as well as the resolved deep convection (Haakenstad et al., 2021; Haakenstad and Breivik, 2022). Still, Haakenstad and Breivik (2022) report at least two biases that may be important for the present study, namely a significant underestimation of spring temperatures as well as too long-lasting snow cover in regions with few observations.

Previous studies that attempted to relate weather data to avalanches note that meteorological parameters *above a certain elevation* are most important regarding avalanche release (e.g. Kronholm et al., 2006; Laute and Beylich, 2018; Dyrørdal et al., 2020). We have conducted our analysis using several different elevation thresholds, selecting grid cells between 400 and 900 m, 500 and 1000, and 600 and 1100 m. However, the choice of elevation threshold had little impact on the final results. The results presented here are based on the elevation interval 400 to 900 m and the number of grid cells selected per region is shown in Table 1.

2.3 seNorge

To obtain more information about the snow conditions the snow model seNorge (Saloranta, 2012) version 1.1.1 (Saloranta, 2014, 2016) is run using NORA3 daily 2-m air temperature and total precipitation amount as input. This model is the “work-horse” for the avalanche warning system in Norway (Morin et al., 2020) and well suited for Norwegian conditions (Saloranta, 2012). It is a simple process-based single-layer snowpack model demanding little computational resources, thus being convenient for application to large high-resolution grids (Saloranta, 2016; Morin et al., 2020). seNorge consists of two sub-modules for (1) snowpack water balance and (2) snow compaction and density, calculating the snow water equivalent, the melt/refreeze rate, and run-off as well as snow depth and density, respectively. To obtain reasonable initialisation data for seNorge, the model was first run for the years 1970 through 1975 with the initial values being zero everywhere. The final simulation outputs from



Table 1. Number of selected grid cells between elevation levels 400 m and 900 m for the NORA3 grid cell selection.

Region	Number of cells
Indre Troms	461
Lyngen	136
Nord-Troms	594
Sør-Troms	146
Tromsø	41

1975 were then used as model initialisation data for 1970 and the model was run from 1970 through 2023 to produce the
225 snow-cover data.

Note that some years ago the much more elaborate snowpack model Crocus was applied in Norway to obtain snowpack
stratigraphy information. However, this was discontinued in the 2017/18 season due to unreliable results and lack of personnel
to maintain the model chain (Morin et al., 2020). Thus, for the time being, the seNorge model represents the best available
gridded snow data for Norway. Efforts are currently underway in cooperation with the Norwegian Water Resources and Energy
230 Directorate (NVE) to implement and run the detailed snowpack model SNOWPACK based on Norwegian data (Karsten Müller,
personal communication). It is planned to incorporate the SNOWPACK simulations into our machine learning system for ADL
prediction when they are available.

2.4 Avalanche-danger prediction features

Based on the NORA3 weather data several parameters are constructed to be used as potential predictors of ADL, partly follow-
235 ing earlier studies (e.g., Hendrikx et al., 2014; Gauthier et al., 2017; Pérez-Guillén et al., 2022). An overview of these potential
predictors is presented in Table 2. They include the accumulated new liquid precipitation r_1 on the day of the ADL assessment,
as well as the new liquid precipitation accumulated over one to six days before and including the day (r_2, \dots, r_7). Equivalently,
solid precipitation is represented by the features s_1, \dots, s_7 . The hourly total precipitation (P_{tot}) values from NORA3 were clas-
sified as liquid or solid based on the hourly 2-m air temperature being larger or smaller than 0°C , respectively. The parameters
240 rh, rh_2, \dots, rh_7 correspond to the to daily and 2-day to 7-day averages of the relative humidity. The maximum and minimum of
2-m air temperature (t_{max}, t_{min}) and 10-m wind speed (w_{max}) represent the daily maximum and minimum of *hourly* values
from NORA3, respectively. The diurnal cycles dtr, dtr_1, dtr_2, dtr_3 represent the difference between the maximum and minimum
hourly 2-m air temperatures on the day of and up to three days before the ADL assessment. The thermal amplitudes $dtrd_1,$
 $dtrd_2, dtrd_3$ represent the largest thermal range of hourly 2-m air temperatures between the day of and one to three days before
245 the assessment. The ftc is a boolean flag indicating if a freeze-thaw cycle was present on the day of the assessment, i.e., if the
daily t_{max} was larger than 0°C and the daily t_{min} was smaller than 0°C . The positive-degree days (pdd) are calculated as the
seven-day sum (including the day of the assessment) of the daily mean 2-m air temperature (t_{mean}) for days with $t_{mean} > 0$



°C. The drift index (w_{drift}) combines precipitation and wind (see Table 2) to represent the effect of snow drift (Hendrikx et al., 2005). The cubed drift index (w_{drift3}) is also included as this is more in line with the current understanding of snow transport
250 by wind (Hendrikx et al., 2014). Further parameters include the net short-wave and long-wave radiation at surface (n_{sw} and n_{lw} , respectively) averaged over one to seven days. As described in section 2.3, we also use parameters generated with the seNorge snow model. These are the snow water equivalent (SWE), snow depth (SDP), snow density (SD), and melt/refreeze rate (MR). The parameters are included as daily and 2-day to up to 7-day means.

The predictive features are calculated for all days for which ADLs are available, covering the period of winter 2017/18 to
255 2022/23. The avalanche period is considered as lasting from December to May, including these months, although in few cases there are ADLs for days in late November and early June. The data is split into a training and a test dataset. To avoid a potential overestimation of model skill due to intra-seasonal correlation, we use the two full avalanche seasons of 2020/21 and 2022/23 as test data and the remaining seasons as training data. The two test seasons are rather different in terms of ADL frequencies (see Fig. 2), thus covering at least some interseasonal variation. When training the statistical models we average the predictive
260 features for each of the five avalanche regions separately (Fig. 1). However, we train *one* model for all five regions combined because there is not enough data to robustly train a statistical model per region (especially for level 4 with only 120 cases for all regions combined; see Fig. 2a). We note that we have tested taking the 90th percentile of the grid cells per region instead of the average, but this had little impact on our final results.

3 Methods

265 In the following we introduce the random forest (RF) model used to predict avalanche danger based on meteorological data and then give a brief summary of the model evaluation metrics. For a description of the artificial neural network (ANN) see text S1 in the online supplementary information.

3.1 Random forest

The random forest (RF; Breiman, 2001) model is a non-linear supervised classifier based on an aggregation of weaker classi-
270 fiers (the decision tree). The decision tree (DT; Breiman et al., 1984) establishes “splitting rules” for the continuous features to predict the discrete target variable (i.e., the ADL). The splitting rules are here obtained by minimising the *Gini index of diversity* (e.g., Breiman et al., 1984):

$$\text{Gini} = \sum_{i=1}^N (p_i (1 - p_i)), \quad (1)$$

where N is the number of classes in the data and p_i is the probability of correctly classifying item i . Higher and lower *Gini*
275 *indices* correspond to greater and smaller misclassification, respectively. The number of splitting rules sets the “depth” of the DT and the user may determine the minimum number of data samples that must remain after a split.



Table 2. Potential predictors constructed from NORA3 meteorological data. The “current day” refers to the day of the avalanche danger assessment. The capitalised abbreviations indicate that the respective parameter was derived with the seNorge model. See the text for more details on the parameter definition.

Feature name	Description
Ptot	Daily total accumulated new precipitation (mm)
r1, ..., r7	Daily to 7-day accumulated new liquid precipitation (mm)
s1, ..., s7	Daily to 7-day accumulated new solid precipitation (mm)
rh, rh2, ..., rh7	Daily to 7-day mean of relative humidity
t1, ..., t7	Daily to 7-day mean temperature (K)
tmin	Daily minimum temperature (K)
tmax, tmax2, ..., 7	Daily to 7-day maximum temperature (K)
dtr	Daily temperature range (K)
dtr1, dtr2, dtr3	Diurnal cycle one to three days before the current day (K)
dtrd1, dtrd2, dtrd3	Thermal amplitude between one to three days before and the current day (K)
ftc	Daily freeze-thaw cycle (ftc = 1)
pdd	Positive-degree days (7-day sum of tmean for days with tmean > 0 °C)
w1, ..., 7	Daily to 7-day mean wind speed (ms ⁻¹)
wmax, wmax2, ..., 7	Daily to 7-day maximum wind speed (ms ⁻¹)
w_dir	Daily wind direction
wdrift	Drift index (w_mean × s1) (ms ⁻¹ × mm)
wdrift3	Cubed drift index (w_mean ³ × s1) (ms ⁻³ × mm)
wdrift_2, 3	As wdrift but mean wind and precipitation sum over two and three days
wdrift3_2, 3	As wdrift3 but mean wind and precipitation sum over two and three days
nsw, nsw2, ..., nsw7	Daily to 7-day mean of net short-wave radiation at surface (Wm ⁻²)
nlw, nlw2, ..., nlw7	Daily to 7-day mean of net long-wave radiation at surface (Wm ⁻²)
SWE, SWE2, ..., SWE7	Daily to 7-day mean of snow water equivalent (mm)
SDP, SDP2, ..., SDP7	Daily to 7-day mean of snow depth (mm)
SD, SD2, ..., SD7	Daily to 7-day mean of snow density (kg/L)
MR, MR2, ..., MR7	Daily to 7-day mean of melt/refreeze rate (mm/d)

The RF grows multiple DTs, and the final outcome (i.e., the ADL based on a specific set of feature values) is obtained by the majority vote of the outcome of the individual DTs. Using a large number of DTs typically helps to prevent overfitting. As another measure to prevent overfitting, the individual DTs are trained on bootstrapped subsets of the data.



280 The RF method offers the possibility to gauge the importance of the individual predictive features in the prediction of the target variable. This is done by computing the average impurity decrease computed across all DTs in the RF due to the respective predictive feature.

Note that while an individual DT may be humanly understandable (given it is not too large), the RF typically consists of hundreds of DTs, meaning it is a “black-box”. However, due to the large number of features (up to 109 features are considered
285 as potential predictors here), a “black-box” model is likely unavoidable for ADL prediction

In the context of the prediction of snow avalanches, the RF method has become quite popular. However, it seems to be mostly used for the prediction of avalanche activity based on avalanche observations (e.g., Möhle et al., 2014; Dkengne Sielenou et al., 2021; Mayer et al., 2023, 2024; Viallon-Galinier et al., 2023) and Pérez-Guillén et al. (2022) appear to be the first applying an RF to ADL prediction.

290 3.2 Model evaluation metrics

To evaluate and compare model performance, several performance metrics (e.g., Sokolova and Lapalme, 2009) are employed, similar to earlier studies (e.g., Fromm and Schönberger, 2022; Pérez-Guillén et al., 2022). We use hits (a), false alarms (b), misses (c), and correct non-events (d) (see Table 3) to calculate the following performance metrics:

$$\text{PC} = \frac{a + d}{a + b + c + d}, \text{ the accuracy or percentage of correctly classified samples,} \quad (2)$$

295

$$\text{P} = \frac{a}{a + b}, \text{ the precision score,} \quad (3)$$

representing the fraction of hits among the positive forecasts (i.e., hits and false alarms),

$$\text{R} = \frac{a}{a + c}, \text{ the recall score,} \quad (4)$$

representing the fraction of hits among the positive observations (i.e., hits and misses), as well as

$$\text{300 F1} = 2 \frac{P \times R}{P + R}, \text{ the F1 score,} \quad (5)$$

which corresponds to the harmonic mean of precision and recall. Following Pérez-Guillén et al. (2022) we use the F1-macro score in the cross-validation during the model optimisation procedure (section 4). A macro score represents the unweighted mean of the score over all classes, thus treating all classes equally (e.g., Sokolova and Lapalme, 2009). As noted by Sokolova and Lapalme (2009), precision, recall, and hence the F1 score are invariant to changes in the classification of correct non-events.

305 4 Random forest optimisation and feature selection

As mentioned above, our focus in this study is the random forest (RF) model, and the model optimisation and feature selection procedure mostly follows Pérez-Guillén et al. (2022). However, note that we here consider both the binary-case levels (BCLs)



Table 3. Structure of the binary confusion matrix (see e.g., Sokolova and Lapalme, 2009; Wilks, 2011).

	obs. positive	obs. negative
forecast positive	a	b
forecast negative	c	d

and the 4-level case ADLs (see section 2.1). Consequently, the optimisation and feature selection procedure is conducted separately for these cases.

310 The RF model is a complex machine-learning method incorporating several hyperparameters which may be tuned to optimise the model. We start by performing a randomised grid search over several hyperparameters using the full set of 109 features (see section 2.4). During the grid search a 3-fold cross-validation is performed employing the F1-macro score (i.e., the unweighted mean of F1 scores for each class) to gauge model performance. Since we have six winters of data available, the folds are constructed such that in each fold four winters are used as training data and the remaining two winters as test data. As the classes
315 of the target variable are strongly imbalanced (see Fig. 2) we use a synthetic minority over-sampling technique (SMOTE; Chawla et al., 2002) to oversample the minority classes and balance the data. Note that in the binary case the balancing was undertaken *after* the aggregation from ADL to BCL. The RF with the set of hyperparameters achieving the best (i.e., highest) F1-macro score is then used to gauge the importance of the individual predictive features as described in section 3.1. In a next step, the cross-correlation (Pearson R) between all the predictive features is calculated. Those features which exhibit $R^2 > 0.9$
320 with another feature of greater importance are then removed. This leaves 54 and 56 features in the binary and the 4-level case, respectively. Their feature importances are shown in Fig. 3. Employing only the remaining 54 and 56 features, we perform another grid search around the best hyperparameters found in the first step. This yields the final set of hyperparameters as shown in Table 4. Finally, we test the optimal number of features to be included. As can be seen in Fig. 4, for the binary case there is a considerable increase in median model performance from 10 to 20 features, while including more than 20 features
325 either does not change or even deteriorates the performance. Hence, we choose 20 features in the binary case. For the 4-level case increasing the number of features from 20 to 30 improves the median performance, but for higher feature numbers the performance deteriorates again. Thus, we choose 30 features for the 4-level case. The features above the black lines in Fig. 3 constitute the final sets of features used in the further analysis. Figure 4 shows the RF performance derived from a 3-fold cross-validation (i.e., using four winters as training and two winters as test data). The same optimal feature numbers are obtained
330 in a 6-fold cross-validation (i.e., using five winters as training and one winter as test data; see Fig. S6 in the supplementary information). Note that Pérez-Guillén et al. (2022) similarly find 30 to be the optimum number of predictive features, although they use different features (including SNOWPACK-derived snow-stratigraphy parameters; compare their Fig. 5 with our Fig. 3b).

Generally, the most important parameters in both the binary and the 4-level case are related to new snow accumulating over
335 several days (e.g., s3, s6) together with snow density (SD4) as well as the wind (e.g., wmax2, w_dir) and wind drift (e.g.,

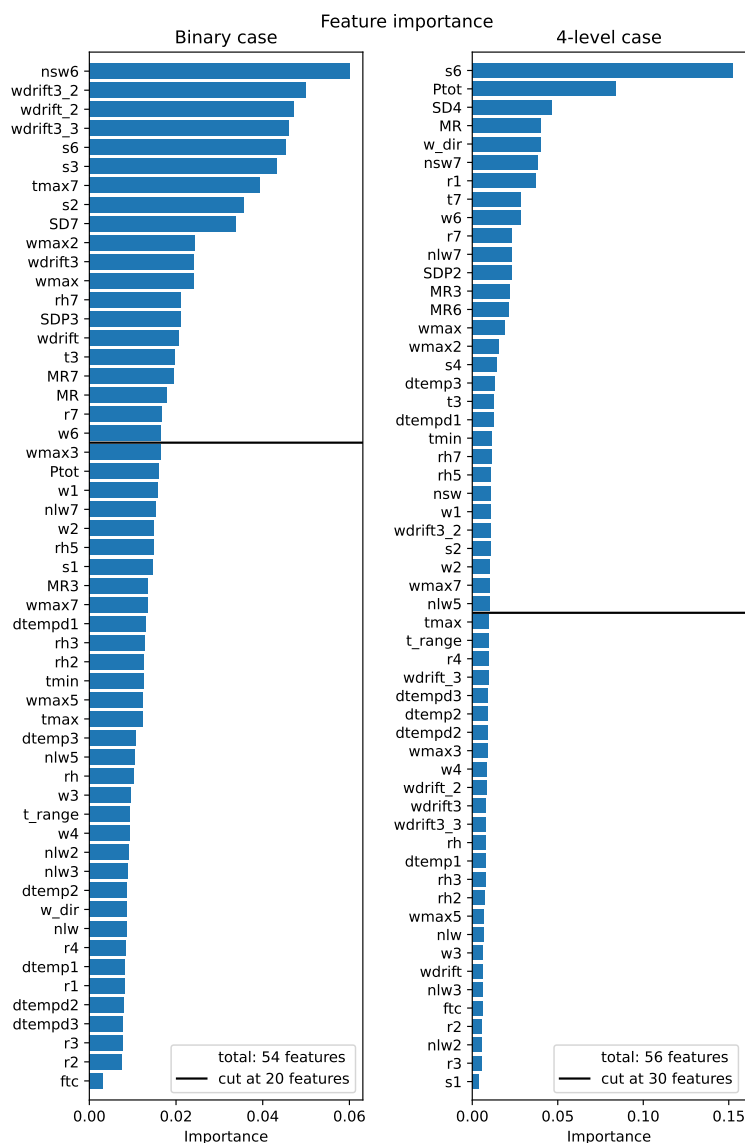


Figure 3. Feature importances for the random forest models trained for (a) the binary case and (b) the 4-level case. The black horizontal lines indicate the cut-off point determined in the optimal feature number test described in the text. For a description of the features see Table 2.

wdrift3_3, wdrift_3). This is expected and broadly consistent with Pérez-Guillén et al. (2022)⁸ as well as other studies which, however, investigate avalanche activity instead of ADL (e.g., Gauthier et al., 2017; Jaedicke et al., 2008; Bakkehøi, 1987; Kronholm et al., 2006; Hao et al., 2023), since both new snow and wind, especially associated with storms (e.g., Davis et al., 1999), are prominent avalanche triggers (see e.g., Jaedicke et al., 2008; Dyrørdal et al., 2020, specifically for northern Norway).

⁸Note that our wdrift parameters appear to correspond to the wind_trans parameters in Pérez-Guillén et al. (2022).



Table 4. The sets of hyperparameters used in the random forest models. The row “Maximum number of features” refers to the number of features considered at each split in the decision trees. “sqrt” indicates the square root of the number of all features and “1.0” indicates all features.

Hyperparameter	binary	4-level
Number of trees	900	500
Maximum depth of the tree	20	35
Maximum number of features	sqrt	1.0
Minimum number of samples at leaf node	9	2
Minimum number of samples for each split	2	4

340 Interestingly, the 6-day and 7-day averaged net short-wave radiation features (nsw6, nsw7) are among the most important
features in the binary and the 4-level case, respectively. This is remarkable, since for most of the northern Norwegian winter
polar-night conditions obtain, meaning the sun does not rise and there is no short-wave radiation. Indeed, while nsw6 never
exceeds 2 Wm^{-2} in winter (December through February), in spring (March through May) typical values are between 40 and
50 Wm^{-2} (see Fig. S7). Accordingly, the importance of nsw6 and nsw7 should be concentrated in the spring months. These
345 parameters are likely related directly to melting and refreezing (e.g., nsw6 and MR6 are highly correlated, see Fig. S8) but
also to clouds. As clouds are connected to precipitation and wind, this partly explains its comparatively high importance.
Furthermore, as documented by, e.g., Conway et al. (1988), on slopes with a southerly aspect, avalanches are often released
after the snow has been warmed by solar radiation. A few features directly related to temperature are among the most important
features, mostly as longer averages (t7, tmax7). However, it is unclear how these temperature features impact avalanche danger
350 since, as noted by e.g. Kronholm et al. (2006), higher temperatures can have both stabilising and destabilising effects on the
snow cover. Higher temperatures may, e.g., lead to more meltwater that can percolate through the snowpack (destabilising),
while they may also decrease the time over which weak layers are present in the snowpack (stabilising). The features related to
temperature *change* (e.g., t_range, dtemp1 etc.) are of minor importance in the 4-level case and are not used in the binary case
at all, indicating that short-term temperature changes (up to three days) are not important for the ADL in our analysis. For the
355 4-level case, some rain-related features are used in the final model. However, their importance is much lower than that of snow
or total precipitation. This indicates that wet-snow avalanches, which are often caused by rain-on-snow events (e.g., Conway
et al., 1988; Heywood, 1988), mostly do not determine the general ADL. As described in section 2.1, we here consider only
the general ADL. Focusing instead on individual avalanche problems would likely lead to a different set of most important
predictive features used in the RF model, being more directly connected to the specific type of avalanche (wind slab, wet snow,
360 etc.).

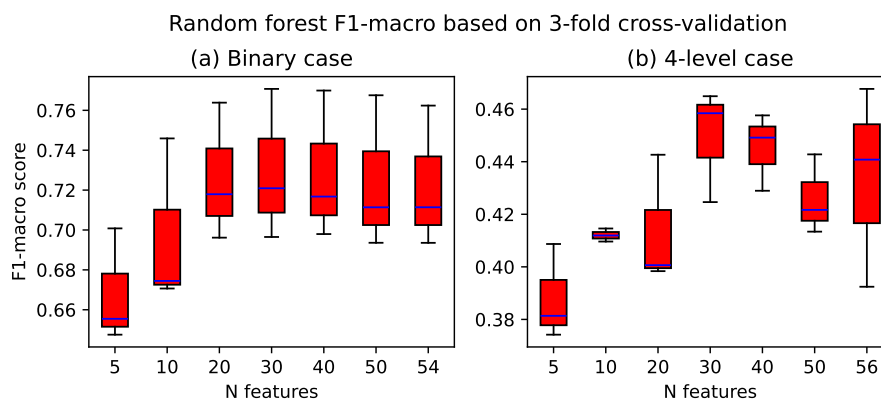


Figure 4. The F1-macro skill score of the random forest dependent on the number of included features based on a 3-fold cross-validation for (a) the binary case and (b) the 4-level case. Note the different y-axis scales. See Fig. S6 in the supplementary information for the results of a 6-fold cross-validation.

Table 5. Classification report for the binary case with unbalanced data. See Table S4 in the supplementary information for the balanced data. For the corresponding classification report of the artificial neural network see Table S1.

level	precision	recall	f1-score	support
0	0.85	0.79	0.82	1227
1	0.62	0.70	0.66	593
accuracy			0.76	1820
macro avg	0.73	0.75	0.74	1820
weighted avg	0.77	0.76	0.77	1820

5 Model evaluation

Summaries of the model performance with respect to the test data (i.e., the winter seasons 2020/21 and 2022/23) for the binary and the 4-level case are presented in Tables 5 and 6, respectively. Heat maps of the corresponding confusion matrices are shown in Fig. 5, and Table 7 gives the difference of the forecast to the true ADL in the 4-level case. See text S2 in the supplementary information for a brief comparison of the performance of the RF and ANN models.

It is clear that in the binary case a much higher overall accuracy of about 76 % is achieved compared to only 57 % in the 4-level case. The latter appears low compared to other studies (Schweizer and Föhn, 1996; Schirmer et al., 2009; Dekanová et al., 2018; Pérez-Guillén et al., 2022; Sharma et al., 2023; Blagovechshenskiy et al., 2023) although it is slightly higher than in Fromm and Schönberger (2022) and Brabec and Meister (2001). Most of these studies used meteorological station data as well as sophisticated information on snow and/or SNOWPACK simulations, which may partly explain their better performance.



Table 6. Classification report for the 4-level case with unbalanced data. See Table S5 in the supplementary information for the balanced data. For the corresponding classification report of the artificial neural network see Table S2.

level	precision	recall	f1-score	support
1	0.42	0.38	0.40	310
2	0.62	0.60	0.61	917
3	0.59	0.63	0.61	563
4	0.22	0.37	0.28	30
accuracy			0.57	1820
macro avg	0.46	0.50	0.48	1820
weighted avg	0.57	0.57	0.57	1820

As previously mentioned, e.g., Sharma et al. (2023) appear to have randomly selected their validation data instead of using whole winters. We note that this has an immense influence on the purported model performance: When we randomly select 33 % of the data as test data, accuracies exceeding 85 % are obtained (both for the binary and the 4-level case). This indicates that strong temporal correlations exist, confounding the model performance when test/validation data are chosen randomly.

375 A further reason for the lower model performance here than, e.g., in Pérez-Guillén et al. (2022) is that they have 20 years of data available and focus only on dry-snow avalanches while we use the general ADL including all avalanche types/problems (see section 2.1). Here we acquiesce to the noisier ADL data to have more training data available for our model, given that our dataset covers only six seasons. However, in future work we will attempt a more detailed analysis with respect to the different avalanche problems. Further reasons may explain (at least in part) the higher accuracies in most of the other studies.

380 For example, Schweizer and Föhn (1996) let a human expert interact with their system, likely increasing the accuracy. Schirmer et al. (2009) used the ADL from the previous day, which increased the model performance. However, since Pérez-Guillén et al. (2022) found that this strongly reduced the model accuracy for days where the ADL changes from the previous day, we here refrain from using the previous-day ADL as predictive feature. As discussed by Fromm and Schönberger (2022), the extent and scale of the investigated region likely also impacts the results. They concentrated on a much smaller region which is more

385 strongly affected by accidental and intentional avalanche release, potentially confounding their results compared to studies focussing, like here, on larger areas (e.g., Pérez-Guillén et al., 2022; Sharma et al., 2023; Schirmer et al., 2009). The region investigated by Dekanová et al. (2018) is smaller than our study area, potentially implying less noisy ADL data, which may explain their somewhat higher model accuracies of 59-66 %.

From Table 5 it appears that our binary-case RF model is better at predicting BCL 0 than 1. However, when the test data

390 are balanced by synthetic oversampling, all three scores (precision, recall, F1) are similar for BCL 0 and 1 (see Table S4 in the supplementary information). Considering the confusion matrix for the 4-level case (Fig. 5b) it is evident that while most of the ADL-2 and ADL-3 cases are classified correctly, ADL 1 is most often misclassified as ADL 2. Most ADL-4 cases are



Table 7. Difference between true and predicted danger level for 4-level case. The numbers given are the percentages of the number of days with the given danger level difference. The left column represents unbalanced and the right column that balanced data. For the corresponding results for the artificial neural network see Table S3.

difference	unbalanced	balanced
-3	0.0	0.0
-2	0.88	0.65
-1	18.02	21.86
0	56.87	58.23
1	23.13	18.38
2	1.04	0.85
3	0.05	0.03

also misclassified as ADL 3. While this means that a large fraction of cases is misclassified, the misclassification difference exceeds one ADL only in about 2 % of cases (see Table 7), which is similar to Pérez-Guillén et al. (2022), and explains the much better model performance in the binary case. However, Pérez-Guillén et al. (2022) generally have smaller differences in misclassification across the different classes, leading to their higher overall accuracy. The left column in Table 7 based on the unbalanced data indicates that our RF model has a tendency to over-predict the ADL, but this is likely due to most cases being either ADL 1 or 2 (Fig. 6) and most ADL-1 cases are misclassified as ADL 2 (Fig. 5b). Accordingly, for the balanced data (Table 7, right column) the situation is reversed, with only a slight underprediction of ADL (see also the confusion matrix for the balanced case in Fig. S9b in the supplementary information). From Fig. 6 it appears that the overall frequencies of the individual ADLs are reproduced in the unbalanced case. However, this is not true for the balanced case, where a severe over-representation of ADLs 2 and 3 is evident, while ADLs 1 and 4 are strongly under-represented. The confusion matrix based on the balanced data (Fig. S9b) shows that about half of the ADL 1 and 4 cases are misclassified as ADL 2 and 3, respectively. This indicates that our RF model has a tendency to over-predict the occurrence of the most frequent classes despite the efforts undertaken to balance the training and cross-validation-test data (see section 4). Another interpretation is that the model over-predicts the frequency of the “medium”-classes (ADLs 2 and 3) at the expense of the more “extreme” classes (ADLs 1 and 4), which may be, at least in part, due to our decision of averaging over multiple grid-cells to generate the predictive features (see section 2.2). However, we have tested taking the 90th percentile instead of the average over the grid cells, but this lead to similar frequencies being predicted for ADLs 2 and 3 (not shown).

6 Hindcasting avalanche danger (1970-2023)

Figure 7 shows the 1970-2023 hindcast of the binary-case avalanche activity (BCA) in the Nord-Troms region. The figures for the other regions are presented in the supplementary information (Fig. S10). The BCA here refers to the number of days

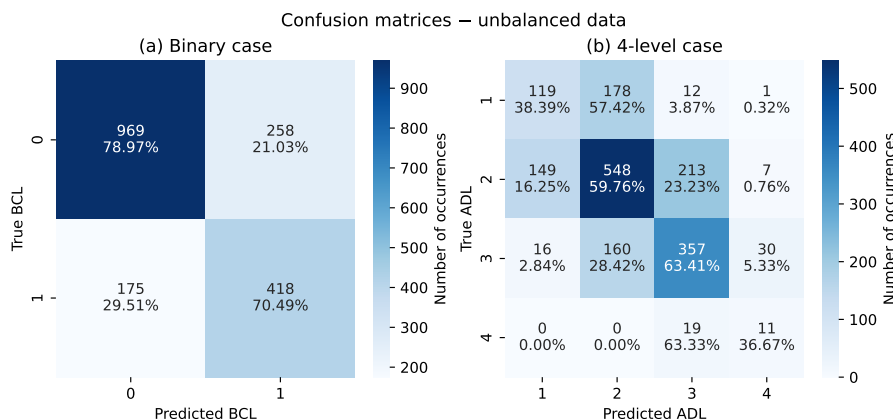


Figure 5. Confusion matrices for the random forest classification with respect to the unbalanced test data for (a) the binary case with binary-case levels (BCL) and (b) the 4-level case with avalanche danger levels (ADL). The values on the diagonals correspond to the recall scores shown in Tables 5 and 6, respectively. For the confusion matrices with respect to the balanced test data see Fig. S9 in the supplementary information. For the corresponding confusion matrices of the artificial neural network see Fig. S1.

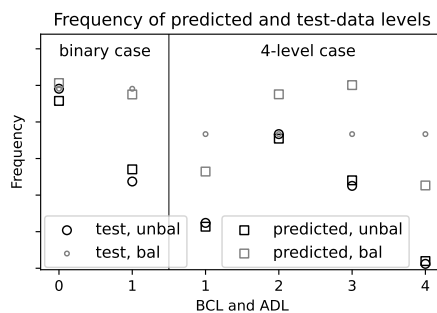


Figure 6. Frequencies of occurrence of (squares) predicted and (circles) test-data danger levels for the (left) binary case with binary-case levels (BCL) and (right) 4-level case with avalanche danger levels (ADL). Shown are both the (black) unbalanced and (gray) balanced data. For the corresponding class frequencies of the artificial neural network see Fig. S2.

per season with a BCL of 1. While the evolution of BCA is not the same in the different regions, there are strong similarities regarding certain features, which may be observed in Fig. 7 and which are briefly summarised in the following. There is little to no trend in the full-season avalanche data from 1970 to 2023 (see Table S6 for linear trends). However, there is a phase of high BCA in the 1990s, mostly due to high BCA in winter (December through February) since the spring (March through May) BCA generally varies less. We note that the increase in BCA in the 1990 is consistent with a simultaneous rise in avalanche activity in Iceland (Keylock, 2003). The phase of high BCA in the 1990s is accompanied by an increase in BCA variance (full season), with a considerable subsequent decrease in variance in 2000-2010, increasing slightly again after 2010. The BCA variance before 1990 is mostly due to spring BCA, as little variance is evident for winter BCA in this period. In the 1990s the

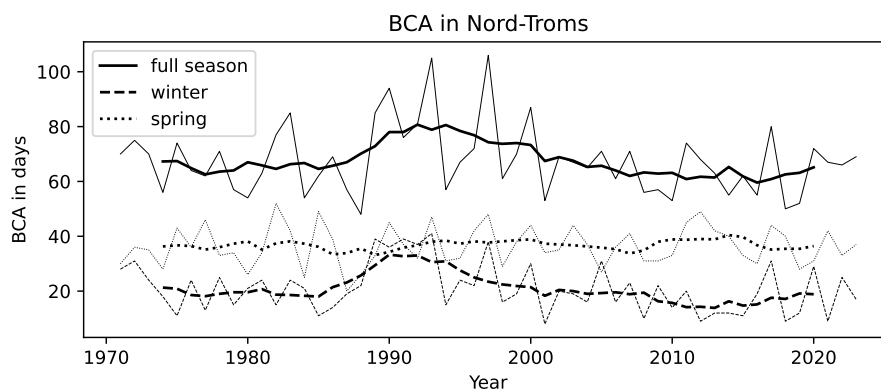


Figure 7. Binary-case avalanche activity (BCA), i.e., the days with level 1 in the binary case, in Nord-Troms for the full season (solid), the winter (dashed), and the spring (dotted) for 1970 to 2023. The thin lines correspond to annual data and the thick lines represent a 7-year rolling mean. See Fig. S10 in the supplementary information for the other regions.

variance in winter and spring appears to be in phase, causing the strong full-season BCA variance. However, in general, spring and winter BCA change in opposite ways over time. In spring there is a small overall increasing trend in BCA, while there is a small decrease in winter. For most of the regions, the spring trends are significant on the 5 % level, while the winter trends are less significant (see Table S6 in the supplementary information).

425 One of the most prevalent features of the BCA hindcast is the peak of winter BCA around 1990 in the 7-year rolling mean which is due to a phase of exclusively high BCA in these years. This is remarkable, since this period is known for exhibiting exceptionally high index values of the North Atlantic Oscillation (NAO; see, e.g., Hurrell, 1995; Wanner et al., 2001) as well as of the Arctic Oscillation (AO; see, e.g., Thompson and Wallace, 1998). The NAO is a measure of the sea-level pressure (SLP) difference between the Icelandic Low and the Azores High and is one of the most well-established climate patterns influencing
430 European climate (e.g., Hurrell, 1995; Wanner et al., 2001)⁹. The AO may be viewed as an extension of the NAO to the whole Northern Hemisphere and interpreted as the surface signature of modulations of the polar vortex at higher elevation (Wanner et al., 2001; Thompson and Wallace, 1998, 2001)¹⁰.

Many studies relate the NAO/AO to the weather conditions in Europe, especially in winter (see, e.g., the review by Wanner et al., 2001). The NAO has also been related specifically to precipitation in northern Europe, including northern Norway, e.g.,
435 by Uvo (2003). This study found that winter precipitation in the Troms region exhibits correlation coefficients with the NAO index of up to 0.5-0.6 (see her Fig. 4). Uvo (2003) also notes that changes in precipitation due to NAO changes are connected to wind and topography. That is, stronger westerly winds induced by a higher NAO index are intercepted by the mountains in the proximity of the Norwegian coast, inducing precipitation there. However, she observes that since the westerly winds generated

⁹The NAO index used here corresponds to the index by Hurrell (1995) which can be downloaded from <https://climatedataguide.ucar.edu/climate-data/hurrell-north-atlantic-oscillation-nao-index-station-based>.

¹⁰The AO data was downloaded from: <https://www.climate.gov/news-features/understanding-climate/climate-variability-arctic-oscillation>.

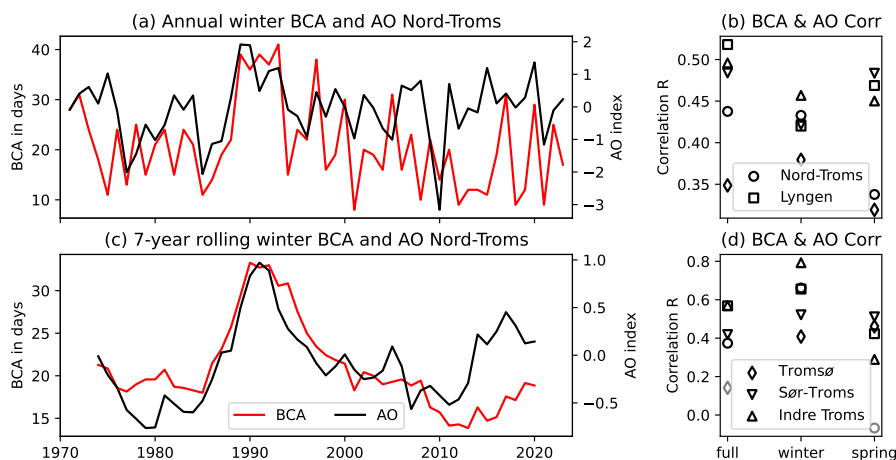


Figure 8. (a) Annual winter hindcast of binary-case avalanche activity (BCA, red) and Arctic Oscillation (AO) index (black) for Nord-Troms. (b) Correlation coefficients of full-season, winter, and spring BCA with AO index for all regions. (c) and (d) are the same as (a) and (b), respectively, but for 7-year rolling means. Black and gray colours in (b) and (d) indicate p values smaller and larger 0.05, respectively, based on a Wald test with a t distribution.

by the Icelandic Low and the Azores High do not reach northern Norway directly, this region is only “intermediately influenced”
 440 by the NAO. Consistently, Rogers (1997) found that North Atlantic storm activity (see also Alexandersson et al., 2000), which
 likely impacts wind and precipitation in northern Europe, is more strongly influenced by low-frequency SLP anomalies in
 the extreme north-eastern Atlantic than by the NAO. This appears to fit the findings of Thompson and Wallace (2001), who
 showed that there is an increase in variance of the North Atlantic storm track associated with a high AO index, meaning that
 more storms reach the far north, inducing stronger winds and more precipitation there. At low AO index, conditions correspond
 445 more to blocking events, preventing storms from reaching further north. Note that the AO index is better correlated with Arctic
 SLP than the NAO index (Fig. S11).

To the authors’ knowledge, the only studies trying to relate the NAO directly to avalanches in Europe are Keylock (2003),
 Jomelli et al. (2007), García et al. (2009), and García-Sellés et al. (2010). The latter two investigated avalanche activity in
 the Pyrenees (north-eastern Spain) and found a negative correlation. Conversely, Jomelli et al. (2007) found no correlation of
 450 avalanche activity and NAO in the French Alps. Finally, Keylock (2003), investigated avalanche activity in Iceland, hence in a
 location more closely related to our region of interest than the other three studies. He tentatively concluded that while the NAO
 may not affect avalanche size distribution, a positive phase of the NAO likely increases avalanche activity.

Consistent with Keylock (2003) and the discussion above regarding the influence of the NAO and AO on northern Nor-
 wegian weather, we find that the northern Norwegian BCA is correlated with both NAO and AO, but more so with the latter
 455 (compare Figs. 8 and S12). The correlation is particularly strong for 7-year rolling means of both quantities, although there is
 considerable variation across the five different regions (Figs. 8d and S13). Notably, Figs. 8b, d, S13, and S14 reveal that while
 the correlations for annual means are not particularly strong ($R=0.35-0.45$), they are more consistent across regions than for

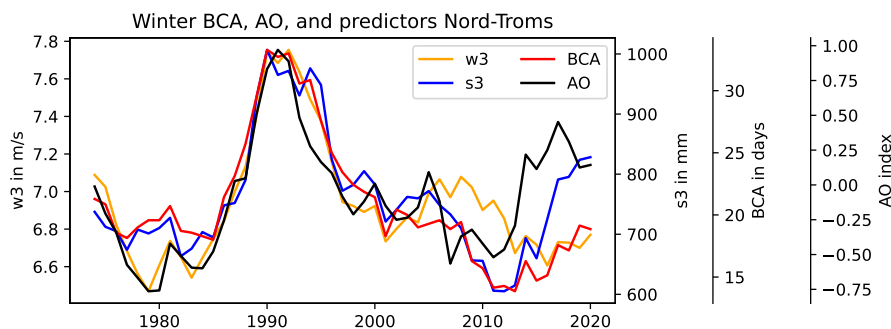


Figure 9. Binary-case avalanche activity (BCA, red), 3-day mean wind speed (w3, orange), and 3-day sum of new snow (s3, blue) in Nord-Troms and Arctic Oscillation (AO) index (black).

the 7-year rolling means ($R=0.4-0.8$), at least in the winter months (December through February). Furthermore, comparing the lead-lag correlations in Figs. S13 and S14 it appears that the clearest correlation between BCA and AO is in the winter months, with a singular peak at AO-lag year 0 for both annual and 7-year rolling means. In the spring months (March through May) there is more variation across regions and while there are correlation peaks at AO-lag year 0, there are further peaks at lead and lag year 4 in the annual means. Thus, we concentrate our further correlation analysis on the winter months.

The 7-year rolling mean time series of winter BCA and AO index show the strong peak in both quantities in the 1990s. Both BCA and AO index decrease subsequently, but while the AO index increases again quite strongly after about 2010, the BCA shows only a small increase. This development obtains in all regions except Indre Troms, where the BCA corresponds more strongly to the AO index (see also the high correlation of of BCA and AO index in this region shown in Fig. 8d).

Since the BCA is here fully determined by the meteorological conditions, we investigate the predictive features and their correspondence with the AO index in the winter months. Figure 9 shows 7-year rolling means of BCA, AO index, and w3 and s3 for Nord-Troms. Note that one of the most important predictive feature in the binary case is `wdrift3_3`, which is a combination of w3 and s3. We choose here to show both components, as the single parameter `wdrift3_3` is more difficult to interpret and may obscure compensating variance of s3 and w3. It is evident that both features follow the AO index quite closely, but while s3 increases with the AO index (with a slight lag) after 2010, w3 does not increase. The discrepancy in the development after 2010 in s3 and w3 likely causes the slower increase in BCA predicted by the RF model. Thus, there is an apparent “decoupling” of wind speed from the AO index after 2010, causing a weakening of the correspondence of BCA and the AO index in most regions. We note that the “decoupling” after 2010 is even stronger for the correspondence of BCA with the NAO index (see Fig. S12c). So far, we have no compelling explanation for this. However, it must be remembered that the AO index is not the only climate mode influencing Scandinavian weather. We have investigated several more climate indices that are important for northern European wind and precipitation and we find that the 7-year rolling mean of the Polar/Eurasian (PE) pattern index shows apparently unprecedented low values in the decade 2010-2020, especially in winter (see Fig. S15). This is remarkable since, as Panagiotopoulos et al. (2002) point out, the PE has a structure similar to the AO. The index representing



another important climate mode, the Scandinavian (SCA) pattern, exhibits consistently high values in winter around 2010 with a subsequent decrease (Fig. S16). A low PE pattern index and a high SCA pattern index have been associated with a weaker polar vortex, likely weakening the westerly winds in the Arctic (e.g., Gao et al., 2017; Panagiotopoulos et al., 2002). Consistently, a higher SCA index has also been associated with weakened storm-track activity over Northern Europe (Bueh
485 and Nakamura, 2007). Hence, the anomalous states of other climate modes may cause the recent apparent “decoupling” of the AO and northern Norwegian wind speed, and thus, the weakening of the correspondence of the AO index with northern Norwegian BCA.

The BCA hindcast with the ANN model is presented in text S3 in the supplementary information. While the results are generally similar we note that the apparent “decoupling” of the BCA from the AO in the last decade is weaker in the ANN-
490 based hindcast (see, e.g., Fig. S5 in the supplementary information). This casts doubts on the robustness of this result and indicates that the influence of the AO on avalanche activity in northern Norway is still uncertain.

7 Summary and conclusions

In this study we implement a machine-learning approach for purely data-driven statistical prediction of avalanche danger level (ADL) based on gridded meteorological (NORA3) and snow (seNorge) information in northern Norway. Two avalanche
495 danger scales are considered: (1) the original ADLs (“4-level case”) and (2) the “binary-case levels” (BCL; “binary-case”) where ADLs 1 and 2 and ADLs 3 and 4 are aggregated to BCL 0 and BCL 1, respectively. For each case a random forest (RF) classifier is optimised and predictive features are selected. The RF model accuracy is considerably higher for the BCLs (76 %) than for the full ADLs (57 %), consistent with the frequent confusion of ADLs 1 and 2 and ADLs 3 and 4 in the latter case. The accuracy in the 4-level case is comparable to or even higher than in some earlier studies (Brabec and Meister, 2001; Fromm and
500 Schönberger, 2022), but lower than in many others (Schirmer et al., 2009; Dekanová et al., 2018; Pérez-Guillén et al., 2022; Sharma et al., 2023; Blagovechshenskiy et al., 2023). We exploit the whole available NORA3 record to perform a hindcast of the binary-case avalanche activity (BCA), which we define as the number of days per season with BCL 1. While there appears to be no general trend there is noticeable variation over time, with a conspicuous peak in BCA in the 1990s, especially in the winter months (December through February). We connect this peak with a well-known Northern Hemispheric climate mode
505 that has been shown to impact European climate, the Arctic Oscillation (AO). The BCA exhibits significant correlation with the AO, especially as a 7-year rolling mean.

Within the last decade, decadal prediction systems have shown an improvement of skill in representing and predicting AO and European winters (e.g., Riddle et al., 2013; Scaife et al., 2014; Kang et al., 2014; Stockdale et al., 2015; Athanasiadis et al., 2017, 2020). Given the here-found connection between BCA and AO, this is encouraging with respect to potential
510 predictability of at least the decadal tendency of avalanche activity in northern Norway. However, the indication that the strength of the connection between the BCA and the AO has weakened in recent years, potentially due to the influence of other climate modes, means that the value of AO predictability for avalanche forecasting remains uncertain.



An important advantage of a fully data-driven approach to predict avalanche danger and activity based on gridded weather/snow data is the potential to generate future projections of those metrics based on climate change scenario simulations (see, e.g.,
515 Castebrunet et al., 2014; Mayer et al., 2024). Such simulations are mostly conducted by global climate models (GCMs) with too coarse resolutions to be usable for avalanche prediction. Thus, regional downscalings are required to produce appropriate data. For Norway such data are available via the Nordic Convection Permitting Climate Projections (NorCP; Lind et al., 2023). In future work we plan to apply our machine-learning model to the NorCP data and generate BCA and ADL projections for northern Norway. However, the likely importance of (regional) climate modes for the development of avalanche activity, as
520 described above, must be taken into account when considering future climate projections. It is not guaranteed that climate modes such as the AO are sufficiently represented in the GCMs and/or NorCP.

As of now the snowpack information for Norway is confined to data based on the simple snow model seNorge. Efforts are currently under way in cooperation with the Norwegian Water Resources and Energy Directorate (NVE) to implement the much more detailed model SNOWPACK to run based on gridded meteorological data. In future research we plan to use the
525 snow-stratigraphy information from SNOWPACK in our machine-learning approach to predict ADL and BCL/BCA. However, we note that results appear to be mixed when it comes to the impact of including SNOWPACK output in ADL prediction machine-learning models: While Schirmer et al. (2009) found an improvement due to the inclusion of SNOWPACK data, the results of Fromm and Schönberger (2022) suggested no improvement. Hence, the impact of the SNOWPACK information on our model performance in Norway remains to be seen.

530 Finally, the ADLs as used here do not distinguish between the different avalanche problems. This likely makes the ADL-data noisy with respect to their relation to meteorological and snow data because different avalanche problems are caused by different weather and snow conditions. Here we opt for the general ADL as it guarantees a larger data set and it aggregates avalanche problems that may be related to similar weather conditions. However, in upcoming research we aim to disentangle the different avalanche problems. The most feasible approach appears to be to select the most frequent avalanche problem to
535 ensure data availability to robustly train a statistical model and at the same time filter some of the “noise” due to the other, less frequent avalanche problems.

High-quality information on avalanche danger is of great importance as it enables stakeholders and people in general to make well-informed decisions affecting their life and property. Our study represents an initial step towards automated avalanche danger prediction in northern Norway that may be used to support and improve expert forecasts. As ongoing and future climate
540 change likely impacts avalanche characteristics, knowledge about potential future changes of these characteristics is valuable. Our methodology can be used to study future changes in avalanche danger and activity based on future-scenario climate-model projections. This information may assist governments and stakeholders in planning of future infrastructure and organisation to prepare for and adapt to environmental conditions in a changing climatic.

Code and data availability. The programming language Python was used to perform the data analysis and generate the figures. The logistic
545 regression and the decision tree were generated using the Python library scikit-learn (Pedregosa et al., 2011). The neural network was



generated with the help of the library Keras (Chollet et al., 2015). The maps were produced with the library Cartopy (Met Office, 2010 - 2024). The code will be made available upon publication.

Author contributions. Kai-Uwe Eiselt and Rune G. Graversen conceived and designed the study. Material preparation, data collection and analysis were performed by Kai-Uwe Eiselt. The first draft of the manuscript was written by Kai-Uwe Eiselt with comments and revisions
550 from Rune G. Graversen.

Competing interests. The authors have no relevant financial or non-financial interests to disclose.

Acknowledgements. The authors thank Debmita Bandyopadhyay, Håvard Thorset, Konstantinos Christakos, and Daniel Krieger for valuable suggestions. We are grateful to Jürg Schweizer for providing us with valuable references and clearing up terminological confusions. Furthermore, we especially thank Christopher D'Amboise for many interesting conversations and suggestions. Finally, we thank Samuel Kočíšček
555 for his help with the Slovak avalanche yearbook. The research is conducted under the IMPETUS project (www.climate-impetus.eu). This project was funded by the European Union's Horizon 2020 research and innovation programme under grant agreement No. 101037084. The random forest models were optimised and trained on the Saga supercomputer at the University of Tromsø (UiT) provided by UNINETT Sigma2, under the project NN9348k.



References

- 560 Alexandersson, H., Tuomenvirta, H., Smith, T., and Iden, K.: Trends of storms in NW Europe derived from an updated pressure data set, *Clim. Res.*, 14, 71–73, <https://doi.org/10.3354/cr014071>, 2000.
- Athanasiadis, P., Bellucci, A., Scaife, A., Hermanson, L., Materia, S., Sanna, A., Borrelli, A., MacLachlan, C., and Gualdi, S.: A multisystem view of wintertime NAO seasonal predictions, *J. Climate*, 30, 1461–1475, <https://doi.org/10.1175/JCLI-D-16-0153.1>, 2017.
- Athanasiadis, P., S. Yeager, Y.-O. K., Bellucci, A., Smith, D. W., and Tibaldi, S.: Decadal predictability of North Atlantic blocking and the NAO, *npj climate and atmospheric science*, 3, 20, <https://doi.org/10.1038/s41612-020-0120-6>, 2020.
- 565 Atwater, M. M.: Snow avalanches, *Sci. Am.*, 190, 26–31, <https://doi.org/10.1038/scientificamerican0154-26>, 1954.
- Bakkehoi, S.: Snow avalanche prediction using a probabilistic method, in: *Avalanche Formation, Movement and Effects*, edited by Salm, B. and Gubler, H., vol. 162 of *Proceedings and Reports*, pp. 549–555, International Association of Hydrological Sciences, available at <https://iahs.info/Publications-News/?category=7>, 1987.
- 570 Bartelt, P. and Lehning, M.: A physical SNOWPACK model for the Swiss avalanche warning Part I: Numerical model, *Cold Reg. Sci. Technol.*, 35, 123–145, [https://doi.org/10.1016/S0165-232X\(02\)00074-5](https://doi.org/10.1016/S0165-232X(02)00074-5), 2002.
- Bengtsson, L., Andrae, U., Aspelien, T., Batrak, Y., Calvo, J., de Rooy, W., Gleeson, E., Hansen-Sass, B., Homleid, M., Hortal, M., Ivarsson, K.-I., Lenderink, G., Niemelä, S., Nielsen, K. P., Onville, J., Rontu, L., Samuelsson, P., Muñoz, D. S., Subias, A., Tijm, S., Toll, V., Yang, X., and Køltzow, M. Ø.: The HARMONIE-AROME Model Configuration in the ALADIN-HIRLAM NWP System, *Mon. Wea. Rev.*, 146, 1919–1935, <https://doi.org/10.1175/MWR-D-16-0417.1>, 2017.
- 575 Blagovechshenskiy, V., Medeu, A., Gulyayeva, T., Zhdanov, V., Ranova, S., Kamalbekova, A., and Aldabergen, U.: Application of Artificial Intelligence in the Assessment and Forecast of Avalanche Danger in the Ile Alatau Ridge, *Water*, 15, 1438, <https://doi.org/10.3390/w15071438>, 2023.
- Brabec, B. and Meister, R.: A nearest-neighbor model for regional avalanche forecasting, *Ann. Glaciol.*, 32, 130–134, <https://doi.org/10.3189/172756401781819247>, 2001.
- 580 Breiman, L.: Random forests, *Mach. Learn.*, 45, 5–32, <https://doi.org/10.1023/A:1010933404324>, 2001.
- Breiman, L., Friedman, J., Stone, C. J., and Olshen, R. A.: *Applied Logistic Regression*, Wadsworth International Group, Belmont, CA, 1984.
- Bueh, C. and Nakamura, H.: Scandinavian pattern and its climatic impact, *Quart. J. Roy. Meteor. Soc.*, 133, 2117–2131, <https://doi.org/10.002/qj.173>, 2007.
- 585 Castebrunet, H., Eckert, N., Giraud, G., Durand, Y., and Morin, S.: Projected changes of snow conditions and avalanche activity in a warming climate: the French Alps over the 2020-2050 and 2070-2100 periods, *The Cryosphere*, 8, 1673–1697, <https://doi.org/10.5194/tc-8-1673-2014>, 2014.
- Chawla, N. V., Bowyer, K. W., Hall, L. O., and Kegelmeyer, W.-P.: SMOTE: Synthetic Minority Over-sampling Technique, *Journal of Artificial Intelligence Research*, 16, 321–357, <https://doi.org/10.1613/jair.953>, 2002.
- 590 Chollet, F. et al.: Keras, <https://keras.io>, 2015.
- Conway, H., Breyfogle, S., and Wilbour, C. R.: Observations relating to wet snow stability, *Proceedings: 1988 International Snow Science Workshop*, Whistler, pp. 211–222, <http://arc.lib.montana.edu/snow-science/item/643>, 1988.



- Davis, R. E., Elder, K., Howlett, D., and Bouzaglou, E.: Relating storm and weather factors to dry slab avalanche activity in Alta, Utah, and Mammoth Mountain, California, using classification and regression trees, *Cold Reg. Sci. Technol.*, 30, 79–89, [https://doi.org/10.1016/S0165-232X\(99\)00032-4](https://doi.org/10.1016/S0165-232X(99)00032-4), 1999.
- Dekanová, M., Duchoň, F., Dekan, M., Kyzek, F., and Biskupič, M.: Avalanche forecasting using neural network, In Proceedings of the IEEE ELEKTRO, Mikulov, Czech Republic, <https://doi.org/10.1109/ELEKTRO.2018.8398359>, 2018.
- Dkengne Sielenou, P., Viallon-Galinier, L., Hagenmuller, P., Naveau, P., Morin, S., Dumont, M., Verfaillie, D., and Eckert, N.: Combining random forests and class-balancing to discriminate between three classes of avalanche activity in the French Alps, *Cold Reg. Sci. Technol.*, 187, 103276, <https://doi.org/10.1016/j.coldregions.2021.103276>, 2021.
- Dyrrdal, A. V., Isaksen, K., and Nilsen, J. K. S. J. I. B.: Present and future changes in winter climate indices relevant for access disruptions in Troms, northern Norway, *Nat. Hazards Earth Syst. Sci.*, 20, 1847–1865, <https://doi.org/10.5194/nhess-20-1847-2020>, 2020.
- Eckerstorfer, M., Malnes, E., and Müller, K.: A complete snow avalanche activity record from a Norwegian forecasting region using Sentinel-1 satellite radar data, *Cold Reg. Sci. Technol.*, 144, 39–51, <https://doi.org/10.1016/j.coldregions.2017.08.004>, 2017.
- Fromm, R. and Schönberger, C.: Estimating the danger of snow avalanches with a machine learning approach using a comprehensive snow cover model, *Mach. Learn. Appl.*, 10, 100405, <https://doi.org/10.1016/j.mlwa.2022.100405>, 2022.
- Gao, T., Yu, J.-Y., and Paek, H.: Impacts of four northern-hemisphere teleconnection patterns on atmospheric circulations over Eurasia and the Pacific, *Theor. Appl. Climatol.*, 129, 815–831, <https://doi.org/10.1007/s00704-016-1801-2>, 2017.
- García, C., Martí, G., Oller, P., Moner, I., Gavalda, J., Martínez, P., and Peña, J. C.: Major avalanches occurrence at regional scale and related atmospheric circulation patterns in the Eastern Pyrenees, *Cold Reg. Sci. Technol.*, 59, 106–118, <https://doi.org/10.1016/j.coldregions.2009.07.009>, 2009.
- García-Sellés, C., Peña, J. C., Martí, G., Oller, P., and Martínez, P.: WeMOI and NAOi influence on major avalanche activity in the Eastern Pyrenees, *Cold Reg. Sci. Technol.*, 64, 137–145, <https://doi.org/10.1016/j.coldregions.2010.08.003>, 2010.
- Gauthier, F., Germain, D., and Héту, B.: Logistic models as a forecasting tool for snow avalanches in a cold maritime climate: northern Gaspésie, Québec, Canada, *Nat Hazards*, 89, 201–232, <https://doi.org/10.1007/s11069-017-2959-3>, 2017.
- Haakenstad, H. and Breivik, Ø.: NORA3. Part II: Precipitation and temperature statistics in complex terrain modeled with a nonhydrostatic model, *J. Appl. Meteor. Climatol.*, 61, 1549–1572, <https://doi.org/10.1175/JAMC-D-22-0005.1>, 2022.
- Haakenstad, H., Breivik, Ø., Furevik, B. R., Reistad, M., Bohlinger, P., and Aarnes, O. J.: NORA3: A nonhydrostatic high-resolution hindcast of the North Sea, the Norwegian Sea, and Barents Sea, *J. Appl. Meteor. Climatol.*, 60, 1443–1464, <https://doi.org/10.1175/JAMC-D-21-0029.1>, 2021.
- Hao, J., Zhang, X., Li, P. C. L., Zhang, G., and Li, C.: Impacts of climate change on snow avalanche activity along a transportation corridor in the Tianshan Mountains, *International Journal of Disaster Risk Science*, 14, 510–522, <https://doi.org/10.1007/s13753-023-00475-0>, 2023.
- Hendrikx, J., Owens, I., Carran, W., and Carran, A.: Avalanche activity in an extreme maritime climate: the application of classification trees for forecasting, *Cold Reg Sci Technol*, 43, 104–116, <https://doi.org/10.1016/j.coldregions.2005.05.006>, 2005.
- Hendrikx, J., Murphy, M., and Onslow, T.: Classification trees as a tool for operational avalanche forecasting on the Seward Highway, Alaska, *Cold Reg Sci Technol*, 97, 113–120, <https://doi.org/10.1016/j.coldregions.2013.08.009>, 2014.
- Hersbach, H., Bell, B., Berrisford, P., Hirahara, S., Horányi, A., Muñoz-Sabater, J., Nicolas, J., Peubey, C., Radu, R., Schepers, D., Simmons, A., Soci, C., Abdalla, S., Abellan, X., Balsamo, G., Bechtold, P., Biavati, G., Bidlot, J., Bonavita, M., Chiara, G. D., Dahlgren, P., Dee, D., Diamantakis, M., Dragani, R., Flemming, J., Forbes, R., Fuentes, M., Geer, A., Haimberger, L., Healy, S., Hogan, R. J., Hólm, E.,



- Janisková, M., Keeley, S., Laloyaux, P., Lopez, P., Lupu, C., Radnoti, G., de Rosnay, P., Rozum, I., Vamborg, F., Villaume, S., and Thépaut, J.-N.: The ERA5 global reanalysis, *Quart. J. Roy. Meteor. Soc.*, 146, 1999–2049, <https://doi.org/10.1002/qj.3803>, 2020.
- Heywood, L.: Rain on snow avalanche events – Some observations, *Proceedings: 1988 International Snow Science Workshop*, Whistler, pp. 125–136, <http://arc.lib.montana.edu/snow-science/item/627>, 1988.
- 635 Hurrell, J. W.: Decadal trends in North Atlantic Oscillation: regional temperatures and precipitation, *Science*, 269, 676–679, <https://doi.org/10.1126/science.269.5224.67>, 1995.
- Jaedicke, C., Solheim, A., Blikra, L. H., Stalsberg, K., Sorteberg, A., Aaheim, A., Kronholm, K., Vikhamar-Schuler, D., Isaksen, K., Sletten, K., Kristensen, K., Barstad, I., Melchiorre, C., Høydal, Ø. A., and Mestl, H.: Spatial and temporal variations of Norwegian geohazards in a changing climate, the GeoExtreme Project, *Nat. Hazards Earth Syst. Sci.*, 8, 893–904, <https://doi.org/10.5194/nhess-8-893-2008>, 2008.
- 640 Jomelli, V., Delval, C., Grancher, D., Escande, S., Brunstein, D., Hetu, B., Filion, L., and Pech, P.: Probabilistic analysis of recent snow avalanche activity and weather in the French Alps, *Cold Reg. Sci. Technol.*, 47, 180–192, <https://doi.org/10.1016/j.coldregions.2006.08.003>, 2007.
- Judson, A. and Erickson, B. J.: Predicting avalanche intensity from weather data: A statistical analysis, US Forest Service research paper RM-112, US Rocky Mountain Forest and Range Experiment Station, Fort Collins, CO, 1973.
- 645 Kang, D., Lee, M.-I., Im, J., Kim, H.-M. K., Kang, H.-S., Schubert, S. D., Arribas, A., and MacLachlan, C.: Prediction of the Arctic Oscillation in boreal winter by dynamical seasonal forecasting systems, *Geophys. Res. Lett.*, 41, 3577–3585, <https://doi.org/10.1002/2014GL060011>, 2014.
- Keylock, C. J.: The North Atlantic Oscillation and snow avalanching in Iceland, *Geophys. Res. Lett.*, 30, 58, <https://doi.org/10.1029/2002GL016272>, 2003.
- 650 Kronholm, K., Vikhamar-Schuler, D., Jaedicke, C., Isaksen, K., Sorteberg, A., and Kristensen, K.: Forecasting snow avalanche days from meteorological data using classification trees; Grasdalen, western Norway, *Proceedings of the 2006 International Snow Science Workshop*, Telluride, Colorado, pp. 786–795, <http://arc.lib.montana.edu/snow-science/item/1016>, 2006.
- LaChapelle, E. R.: Avalanches - A modern synthesis, *Int. Assoc. Hydrol. Sci.*, 69, 75–84, 1966.
- LaChapelle, E. R.: The fundamental processes in conventional avalanche forecasting, *J. Glaciol.*, 26, 75–84, <https://doi.org/10.3189/S0022143000010601>, 1980.
- 655 Laute, K. and Beylich, A. A.: Potential effects of climate change on future snow avalanche activity in western Norway deduced from meteorological data, *Geografiska Annaler: Series A, Physical Geography*, 10, 163–184, <https://doi.org/10.1080/04353676.2018.1425622>, 2018.
- Lehning, M., Bartelt, P., Brown, B., and Fierz, C.: A physical SNOWPACK model for the Swiss avalanche warning: Part III. Meteorological forcing, thin layer formation and evaluation, *Cold Reg. Sci. Technol.*, 35, 169–184, [https://doi.org/10.1016/S0165-232X\(02\)00073-3](https://doi.org/10.1016/S0165-232X(02)00073-3), 2002a.
- 660 Lehning, M., Bartelt, P., Brown, B., Fierz, C., and Satyawali, P.: A physical SNOWPACK model for the Swiss avalanche warning: Part II. Snow microstructure, *Cold Reg. Sci. Technol.*, 35, 147–167, [https://doi.org/10.1016/S0165-232X\(02\)00072-1](https://doi.org/10.1016/S0165-232X(02)00072-1), 2002b.
- Lind, P., Belušić, D., Médus, E., Dobler, A., Pedersen, R. A., Wang, F., Matte, D., Kjellström, E., Landgren, O., Lindstedt, D., Christensen, O. B., and Christensen, J. H.: Climate change information over Fenno-Scandinavia produced with a convection-permitting climate model, *Climate Dyn.*, 61, 519–541, <https://doi.org/10.1007/s00382-022-06589-3>, 2023.
- Maissen, A., Techel, F., and Volpi, M.: A three-stage model pipeline predicting regional avalanche danger in Switzerland (RAvaFcast v1.0.0): a decision-support tool for operational avalanche forecasting, *EGUsphere [preprint]*, <https://doi.org/10.5194/egusphere-2023-2948>, 2024.



- Mayer, S., Techel, F., Schweizer, J., and van Herwijnen, A.: Prediction of natural dry-snow avalanche activity using physics-based snowpack
670 simulations., *Nat. Hazards Earth Syst. Sci.*, 23, 3445–3465, <https://doi.org/10.5194/nhess-23-3445-2023>, 2023.
- Mayer, S., Hendrick, M., Michel, A., Richter, B., Schweizer, J., Wernli, H., and van Herwijnen, A.: Changes in snow avalanche activity in
response to climate warming in the Swiss Alps, *EGUsphere* [preprint], <https://doi.org/10.5194/egusphere-2024-1026>, 2024.
- Met Office: Cartopy: a cartographic python library with a Matplotlib interface, Exeter, Devon, <https://scitools.org.uk/cartopy>, 2010 - 2024.
- Möhle, S., Bründl, M., and Beierle, C.: Modeling a system for decision support in snow avalanche warning using balanced random forest
675 and weighted random forest, in: *International Conference on Artificial Intelligence: Methodology, Systems, and Applications*, edited by
Agre, G., Hitzler, P., Krisnadhi, A. A., and Kuznetsov, S. O., pp. 81–91, Springer, Cham, https://doi.org/10.1007/978-3-319-10554-3_8,
2014.
- Morin, S., Horton, S., Techel, F., Bavay, M., Coléou, C., Fierz, C., Gobiet, A., Hagenmuller, P., Lafaysse, M., Ližar, M., and Mitterer, C.: Ap-
plication of physical snowpack models in support of operational avalanche hazard forecasting: A status report on current implementations
680 and prospects for the future, *Cold Reg. Sci. Technol.*, 170, 102910, <https://doi.org/10.1016/j.coldregions.2019.102910>, 2020.
- Müller, K., Mitterer, C., Engeset, R., Ekker, R., and Kosberg, S.: Combining the conceptual model of avalanche hazard with the Bavar-
ian matrix, *International Snow Science Workshop 2016 Proceedings*, Breckenridge, CO, USA, pp. 472–479, [http://arc.lib.montana.edu/
snow-science/item/2309](http://arc.lib.montana.edu/snow-science/item/2309), 2016a.
- Müller, K., Stucki, T., Mitterer, C., Nairz, P., Konetschny, H., Feistl, T., Coleou, C., Berbenni, F., and Chiambretti, I.: Towards an improved
685 European auxiliary matrix for assessing avalanche danger levels, *International Snow Science Workshop 2016 Proceedings*, Breckenridge,
CO, USA, pp. 1229–1231, <http://arc.lib.montana.edu/snow-science/item/2445>, 2016b.
- Müller, K., Eckerstorfer, M., Grahn, J., Malnes, E., Humstad, R. E. T., and Widforss, A.: Norway’s operational avalanche activity mon-
itoring system using Sentinel-1, in: *2021 IEEE International Geoscience and Remote Sensing Symposium IGARSS*, pp. 236–238,
<https://doi.org/10.1109/IGARSS47720.2021.9553152>, 2021.
- 690 Müller, K., Techel, F., Mitterer, C., Feistl, T., Sofia, S., Roux, N., Palmgren, P., Bellido, G. M., and Bertranda, L.: The EAWS Matrix, a look-
up table for regional avalanche danger level assessment, and its underlying concept, *International Snow Science Workshop Proceedings
2023*, Bend, Oregon, pp. 540–546, <http://arc.lib.montana.edu/snow-science/item/2930>, 2023.
- Panagiotopoulos, F., Shahgedanova, M., and Stephenson, D.: A review of Northern Hemisphere winter-time teleconnection patterns, *J. de
Physique*, 12, 27–47, <https://doi.org/10.1051/jp4:20020450>, 2002.
- 695 Pedregosa, F., Varoquaux, G., Gramfort, A., Michel, V., Thirion, B., Grisel, O., Blondel, M., Prettenhofer, P., Weiss, R., Dubourg, V.,
Vanderplas, J., Passos, A., Cournapeau, D., Brucher, M., Perrot, M., and Duchesnay, E.: Scikit-learn: Machine Learning in Python, *Journal
of Machine Learning Research*, 12, 2825–2830, 2011.
- Pérez-Guillén, C., Techel, F., Hendrick, M., Volpi, M., van Herwijnen, A., Olevski, T., Obozinski, G., Pérez-Cruz, F., and Schweizer, J.:
Data-driven automated predictions of the avalanche danger level for dry-snow conditions in Switzerland, *Nat. Hazards Earth Syst. Sci.*,
700 22, 2031–2056, <https://doi.org/10.5194/nhess-22-2031-2022>, 2022.
- Reistad, M., Breivik, Ø., Haakenstad, H., Aarnes, O. J., Furevik, B. R., and Bidlot, J.: A high-resolution hindcast of wind and waves for the
North Sea, the Norwegian Sea, and the Barents Sea, *J. Geophys. Res.*, 116, C05019, <https://doi.org/10.1029/2010JC006402>, 2011.
- Riddle, E. E., Butler, A. H., Furtado, J. C., Cohen, J. L., and Kumar, A.: CFSv2 ensemble prediction of the wintertime Arctic Oscillation,
Climate Dyn., 41, 1099–1116, <https://doi.org/10.1007/s00382-013-1850-5>, 2013.
- 705 Rogers, J. C.: North Atlantic Storm Track Variability and Its Association to the North Atlantic Oscillation and Climate Variability of Northern
Europe, *J. Climate*, 10, 1635–1647, [https://doi.org/10.1175/1520-0442\(1997\)010<1635:NASTVA>2.0.CO;2](https://doi.org/10.1175/1520-0442(1997)010<1635:NASTVA>2.0.CO;2), 1997.



- Saloranta, T. M.: Simulating snow maps for Norway: description and statistical evaluation of the seNorge snow model, *The Cryosphere*, 6, 1323–1337, <https://doi.org/10.5194/tc-6-1323-2012>, 2012.
- Saloranta, T. M.: Simulating more accurate snow maps for Norway with MCMC parameter estimation method, *Cryosphere Discuss.*, 8, 1973–2003, <https://doi.org/10.5194/tcd-8-1973-2014>, 2014.
- 710 Saloranta, T. M.: Operational snow mapping with simplified data assimilation using the seNorge snow model, *J. Hydrol.*, 538, 314–325, <https://doi.org/10.1016/j.jhydrol.2016.03.061>, 2016.
- Scaife, A. A., Arribas, A., Blockley, E., Brookshaw, A., Clark, R. T., Dunstone, N., Eade, R., Fereday, D., Folland, C. K., M. Gordon, L. H., Knight, J. R., Lea, D. J., MacLachlan, C., Maidens, A., Martin, M., Peterson, A. K., Smith, D., Vellinga, M., Wallace, E., Waters, J., and Williams, A.: Skillful long-range prediction of European and North American winters, *Geophys. Res. Lett.*, 41, 2514–2519, 715 <https://doi.org/10.1002/2014GL059637>, 2014.
- Schirmer, M., Lehning, M., and Schweizer, J.: Statistical forecasting of regional avalanche danger using simulated snow-cover data, *J. Glaciol.*, 55, 761–768, <https://doi.org/10.3189/002214309790152429>, 2009.
- Schweizer, J. and Föhn, P. M. B.: Avalanche forecasting – an expert system approach, *J. Glaciol.*, 42, 318–332, 720 <https://doi.org/10.3189/S0022143000004172>, 1996.
- Schweizer, J., Mitterer, C., Reuter, B., and Techel, F.: Snow avalanche formation, *Rev. Geophys.*, 41, 1016, <https://doi.org/10.1029/2002RG000123>, 2003.
- Schweizer, J., Mitterer, C., Reuter, B., and Techel, F.: On the relation between avalanche occurrence and avalanche danger level, *The Cryosphere*, 14, 737–750, <https://doi.org/10.5194/tc-14-737-2020>, 2020.
- 725 Sharma, V., Kumar, S., and Sushil, R.: A neural network model for automated prediction of avalanche danger level., *Nat. Hazards Earth Syst. Sci.*, 23, 2523–2550, <https://doi.org/10.5194/nhess-23-2523-2023>, 2023.
- Sokolova, M. and Lapalme, G.: A systematic analysis of performance measures for classification tasks, *Inform. Proc. Manage.*, 45, 427–437, <https://doi.org/10.1016/j.ipm.2009.03.002>, 2009.
- Statham, G.: Avalanche hazard, danger and risk—A practical explanation, *Proceedings, International Snow Science Workshop, Whistler, BC*, pp. 224–227, https://arc.lib.montana.edu/snow-science/objects/P__8153.pdf, 2008.
- 730 Statham, G., Haegeli, P., Greene, E., Birkeland, K., Israelson, C., Tremper, B., Stethem, C., McMahon, B., White, B., and Kelly, J.: A conceptual model of avalanche hazard, *Nat. Hazard*, 90, 663–691, <https://doi.org/10.1007/s11069-017-3070-5>, 2018.
- Stockdale, T. N., Molteni, F., and Ferranti, L.: Atmospheric initial conditions and the predictability of the Arctic Oscillation, *Geophys. Res. Lett.*, 42, 1173–1179, <https://doi.org/10.1002/2014GL062681>, 2015.
- 735 Techel, F. and Schweizer, J.: On using local avalanche danger level estimates for regional forecast verification, *Cold Reg. Sci. Technol.*, 144, 52–62, <https://doi.org/10.1016/j.coldregions.2017.07.012>, 2017.
- Thompson, D. W. J. and Wallace, J. M.: The Arctic oscillation signature in the wintertime geopotential height and temperature fields, *Geophys. Res. Lett.*, 25, 1297–1300, <https://doi.org/10.1029/98GL00950>, 1998.
- Thompson, D. W. J. and Wallace, J. M.: Regional Climate Impacts of the Northern Hemisphere Annular Mode, *Science*, 293, 1297–1300, 740 <https://doi.org/10.1126/science.1058958>, 2001.
- Uvo, C. B.: Analysis and regionalization of northern European winter precipitation based on its relationship with the North Atlantic oscillation, *Int. J. Climatol.*, 23, 1185–1194, <https://doi.org/10.1002/joc.930>, 2003.
- Viallon-Galinier, L., Hagenmuller, P., and Eckert, N.: Combining modelled snowpack stability with machine learning to predict avalanche activity, *The Cryosphere*, 17, 2245–2260, <https://doi.org/10.5194/tc-17-2245-2023>, 2023.



- 745 Wanner, H., Brönnimann, S., Casty, C., Gyalistras, D., Luterbacher, J., Schmutz, C., Stephenson, D. B., and Xoplaki, E.: North Atlantic Oscillation – Concepts And Studies, *Surveys in Geophysics*, 22, 321–381, <https://doi.org/10.1023/A:1014217317898>, 2001.
- Wilks, D. S.: *Statistical methods in the atmospheric sciences*, Academic Press, Oxford, UK, 3rd edn., 2011.